

ESI

# **Halogen bonded supramolecular porous structures with kgm layer**

Fujun Cheng<sup>a</sup>, Haijun Wang<sup>a</sup>, Yinying Hua<sup>a</sup>, Haifei Cao<sup>a</sup>, Bihang Zhou<sup>a</sup>, Jingui Duan<sup>\*a, b,</sup>  
<sup>c</sup> and Wanqin Jin<sup>\*a</sup>

<sup>a</sup> State Key Laboratory of Materials-Oriented Chemical Engineering, College of  
Chemical engineering, Nanjing Tech University, Nanjing 210009, China.

<sup>b</sup> Jiangsu National Synergetic Innovation Center for Advanced Materials, Nanjing  
Tech University, Nanjing, 210009, China

<sup>c</sup> State Key Laboratory of Coordination Chemistry, Nanjing University, Nanjing,  
210023, China

**General Procedures and Materials.** All the reagents and solvents were commercially available and used as received. The elemental analysis was carried out with a Perkin-Elmer 240C elemental analyzer. The FTIR spectra were recorded from KBr pellets in the range of 4000-400  $\text{cm}^{-1}$  on a VECTOR 22 spectrometer. Thermal analyses were performed on a Universal V3.9A TA Instruments from room temperature to 700°C with a heating rate of 10°C/min under flowing nitrogen. The powder X-ray diffraction patterns (PXRD) measurements were carried on a Bruker axs D8 Advance 40kV, 40mA for  $\text{CuK}\alpha$  ( $\theta = 1.5418 \text{ \AA}$ ) with a scan rate of 0.2 s/deg at room temperature. Simulated powder patterns from single-crystal X-ray diffraction data were generated using Mercury 1.4.2 software. IR was collected using a Thermo Scientific Nicolet 6700 FTIR spectrometer.

**Synthesis of Br-NTU-16 and I-NTU-16.** The same process was employed to prepare these two structures except replacing the organic linkers. So, only Br-NTU-16 was described in details. Synthesis of Br-NTU-16: copper(II) nitrate (20 mg),  $\text{H}_2\text{L}$ , 12 mg) and  $\text{HNO}_3$  (5  $\mu\text{L}$ ) were mixed with 1.3 mL of  $\text{DMF}/\text{H}_2\text{O}(1:2)$  in a 4 mL glass container and tightly capped with a Teflon vial and heated at 60°C for one day. After temperature cooling down, the resulting high yield green crystals were harvested and washed with DMF. Yield: 74%, based on ligand. Yield: 53% (based on  $\text{H}_2\text{L}$ ). Anal. Calcd for evacuated samples of Br-NTU-16 ( $\text{C}_{24}\text{H}_9\text{Br}_3\text{Cu}_3\text{O}_{12}$ ) C, 31.34; H, 0.99; Found: C, 31.12; H, 1.18. For I-NTU-16 ( $\text{C}_{24}\text{H}_9\text{I}_3\text{Cu}_3\text{O}_{12}$ ) C, 27.18; H, 0.86; Found: C, 26.89; H, 1.21.

### Crystal information

**Single crystal X-ray studies.** Single-crystal X-ray diffraction data were measured on a Bruker Smart Apex CCD diffractometer at 293 K using graphite monochromated  $\text{Mo}/\text{K}\alpha$  radiation ( $\lambda = 0.71073 \text{ \AA}$ ). Data reduction was made with the Bruker Saint program. The crystal of NJU-Bai3 was mounted in a flame sealed capillary containing a small amount of mother liquor to prevent desolvation during data collection, and data were collected at 298K. The structure was solved by direct methods and refined

using the full-matrix least squares technique using the SHELXTL package<sup>1</sup>. Nonhydrogen atoms were refined with anisotropic displacement parameters during the final cycles. Organic hydrogen atoms were placed in calculated positions with isotropic displacement parameters set to 1.2Ueq of the attached atom. The unit cell includes a large region of disordered solvent molecules, which could not be modeled as discrete atomic sites. We employed PLATON/SQUEEZE<sup>2</sup> to calculate the diffraction contribution of the solvent molecules and, thereby, to produce a set of solvent-free diffraction intensities; the structure was then refined again using the data generated.

### Sample activation

The solvent-exchanged sample was prepared by immersing the as synthesized samples in EtOH to remove the nonvolatile solvates, and the extract was decanted every 6 hours and fresh EtOH was replaced. The completely activated sample was obtained by heating the solvent-exchanged sample at room temperature for 6h, 60°C for 6h, and then, 80 °C for 12 h under a dynamic high vacuum.

### Estimation of the isosteric heats of gas adsorption

A virial-type expression comprising the temperature-independent parameters  $a_i$  and  $b_i$  was employed to calculate the enthalpies of adsorption for CO<sub>2</sub> on Br-NTU-16 and I-NTU-16<sup>3</sup>. In each case, the data were fitted using the equation:

$$\ln P = \ln N + 1/T \sum_{i=0}^m a_i N^i + \sum_{i=0}^n b_i N^i \quad (1)$$

Here,  $P$  is the pressure expressed in Torr,  $N$  is the amount adsorbed in mmol/g,  $T$  is the temperature in K,  $a_i$  and  $b_i$  are virial coefficients, and  $m$ ,  $n$  represent the number of coefficients required to adequately describe the isotherms ( $m$  and  $n$  were gradually increased until the contribution of extra added  $a$  and  $b$  coefficients was deemed to be statistically insignificant towards the overall fit, and the average value of the squared deviations from the experimental values was minimized).

$$Q_{st} = -R \sum_{i=0}^m a_i N^i \quad (2)$$

Here,  $Q_{st}$  is the coverage-dependent isosteric heat of adsorption and  $R$  is the

universal gas constant.

From these results, the Henry's constant ( $K_H$ ) is calculated from where  $T$  is temperature.

$$K_H = \exp(-b_0) \cdot \exp(-a_0 / T) \quad (3)$$

The Henry's Law selectivity for gas component  $i$  over  $j$  at 273 and 298 K were calculated based on Eq. 4.

$$S_{ij} = K_{Hi} / K_{Hj} \quad (4)$$

**Table S1.** Crystal data and structure refinement for Br-NTU-16 and I-NTU-16

	Br-NTU-16	I-NTU-16
Empirical formula	C <sub>24</sub> H <sub>15</sub> Br <sub>3</sub> Cu <sub>3</sub> O <sub>15</sub>	C <sub>24</sub> H <sub>15</sub> I <sub>3</sub> Cu <sub>3</sub> O <sub>15</sub>
Formula weight	973.7	1114.71
Crystal system	monoclinic	monoclinic
Space group	<i>C2/m</i>	<i>C2/m</i>
Unit cell dimensions	<i>a</i> = 14.042(9) Å <i>b</i> = 18.453(11) Å <i>c</i> = 17.330(11) Å <i>β</i> = 110.124(7)°	<i>a</i> = 14.453(14) Å <i>b</i> = 18.753(18) Å <i>c</i> = 17.444(17) Å <i>β</i> = 110.169(11)°
Volume	4216(4) Å <sup>3</sup>	4438(7) Å <sup>3</sup>
Z	4	4
Density (calculated)	1.532 g/cm <sup>3</sup>	1.668 g/cm <sup>3</sup>
Mu(MoKa)	4.394 mm <sup>-1</sup>	3.560 mm <sup>-1</sup>
F(000)	1880	2100
Theta min-max	1.251, 25.05	1.251, 25.05
Index ranges	-16 ≤ <i>h</i> ≤ 16 -19 ≤ <i>k</i> ≤ 21 -20 ≤ <i>l</i> ≤ 20	-17 ≤ <i>h</i> ≤ 17 -22 ≤ <i>k</i> ≤ 22 -20 ≤ <i>l</i> ≤ 20
Tot., Uniq. Data, R(int)	14678, 3852, 0.184	15448, 4045, 0.153
Observed data [ <i>I</i> > 2σ( <i>I</i> )]	1726	2457
Nref, Npar	3852, 212	4045, 211
R <sub>1</sub> , wR <sub>2</sub> , S	0.0867, 0.1909, 1.02	0.0664, 0.1876, 0.99
Max Shift	0	0

$$R = \sum ||F_o| - |F_c|| / \sum |F_o|, wR = \{\sum [w(|F_o|^2 - |F_c|^2)^2] / \sum [w(|F_o|^4)]\}^{1/2} \text{ and } w = 1/[\sigma^2(F_o^2) + (0.1452P)^2] \text{ where } P = (F_o^2 + 2F_c^2)/3$$

**Table S2.** X-ray crystallographically determined O–Br bond distances and C–Br–O bond angles for NTU-16.

	r (O-Br) (Å)	$\sigma$ (O-Br-C) (°)	d (O-C) (Å)	d (Br-C) (Å)
C4-Br1...O2	3.194	171.28	5.115	1.931
C6-I1...O4	3.198	170.73	5.311	2.130

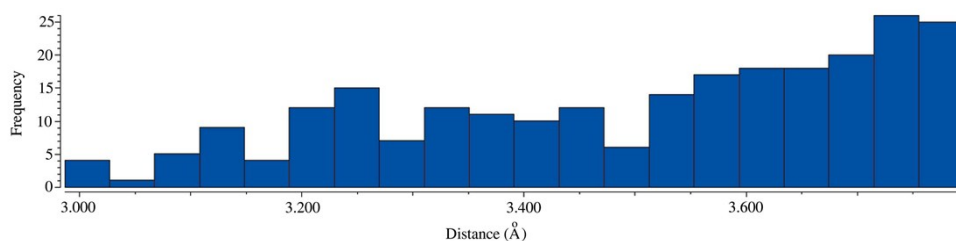
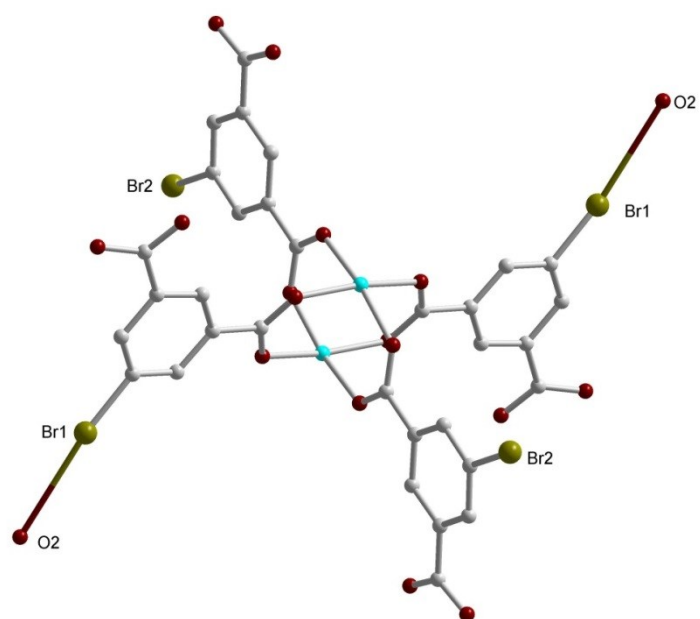
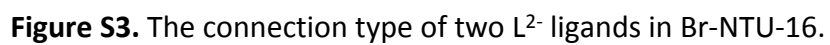
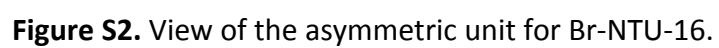
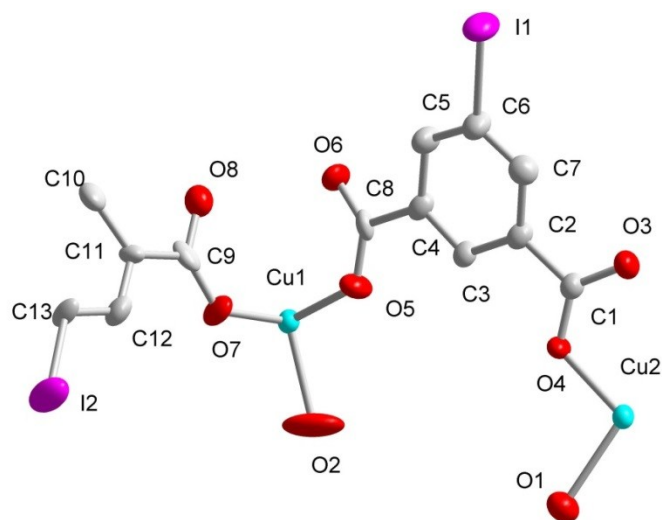


Figure S1 Histogram comparing the lengths of intermolecular Br...O contacts within the range 2.8–3.8 Å in compounds with Br- and methoxy-substituted benzene rings<sup>4</sup>.



**Figure S4.** Halogen bonds of Br1...O2 in NTU-16.



**Figure S5.** View of the asymmetric unit for I-NTU-16.

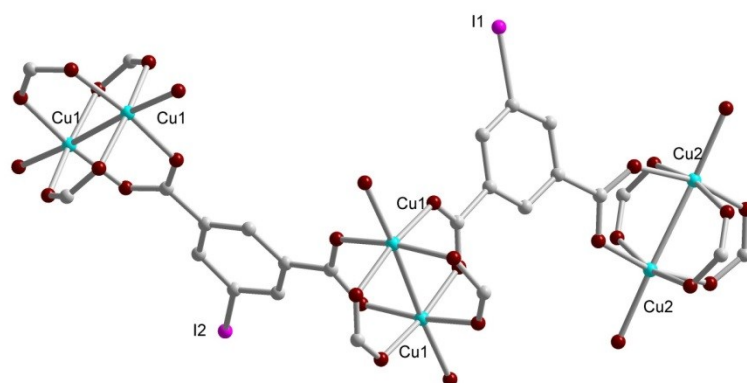


**Figure S6.** The connection type of two  $L^{2-}$  ligands in I-NTU-16.

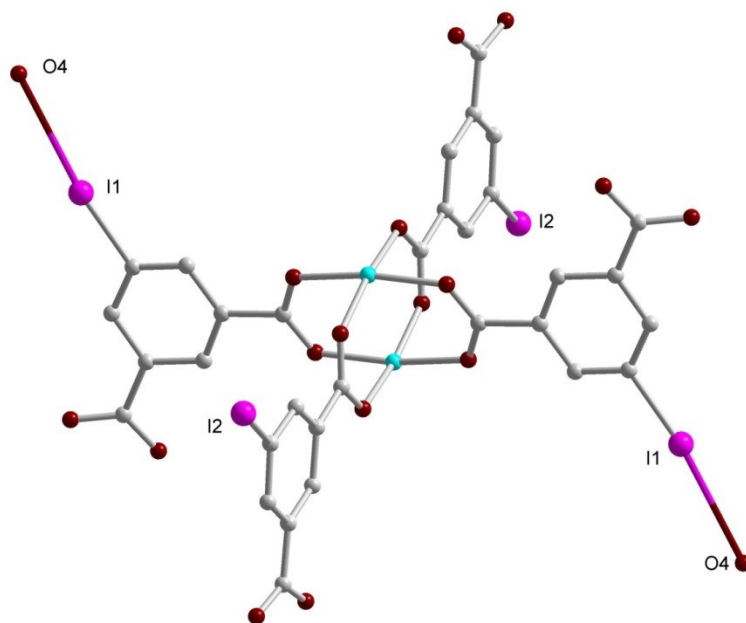




**Figure S7.** Halogen bonds of I1...O4 in NTU-16.

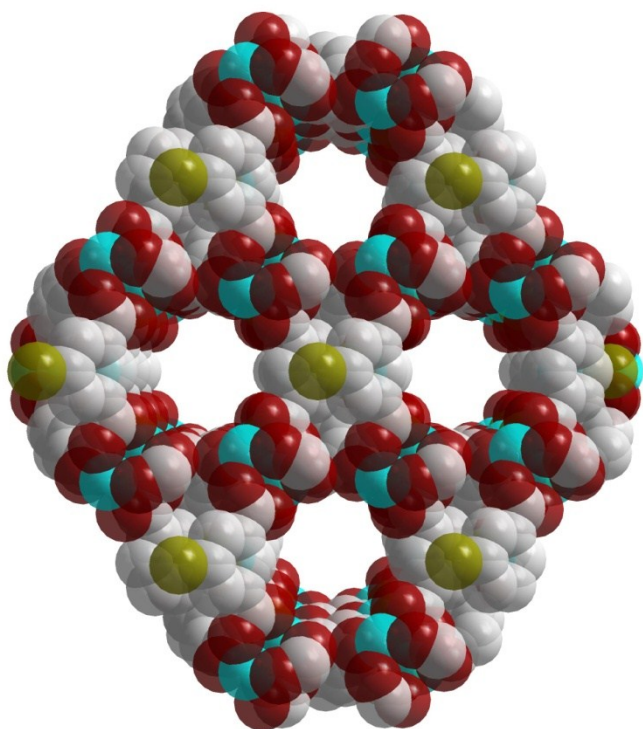


**Figure S8.** The packing view of accessible pore volume of Br-NTU-16 along *c*-axis

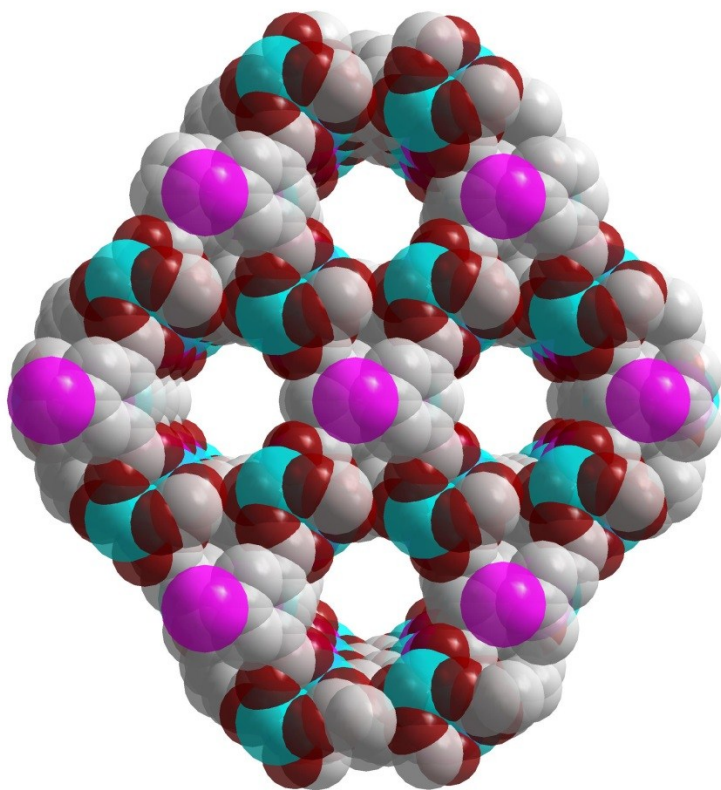


**Figure S9.** The packing view of accessible pore volume of I-NTU-16 along *c*-axis

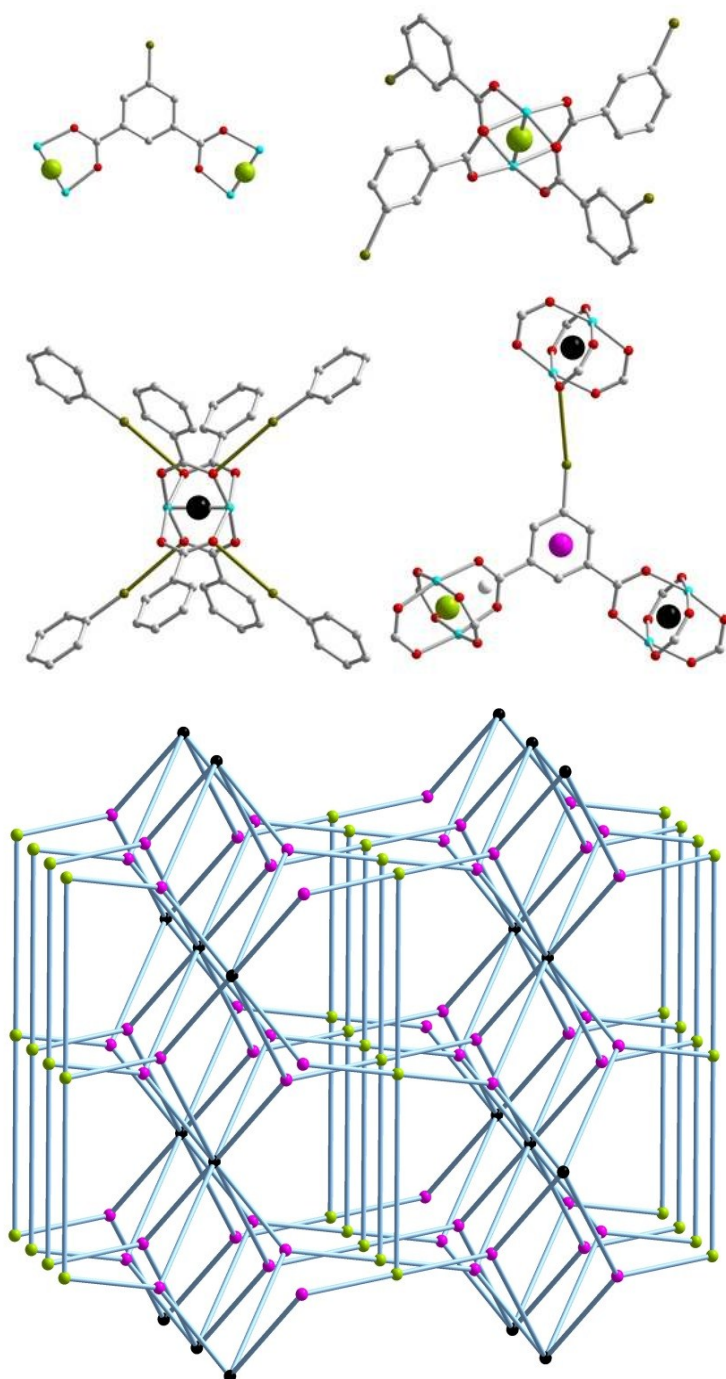


**Figure S10.** The simplified topology 3,4,8-c net of Br-NTU-16 and I-NTU-16: Point symbol for net:  $\{4.5^2\}_4\{4^4.4.5^4.7^4.8^4.12.10^4\}\{5^4.8^2\}_2$ .

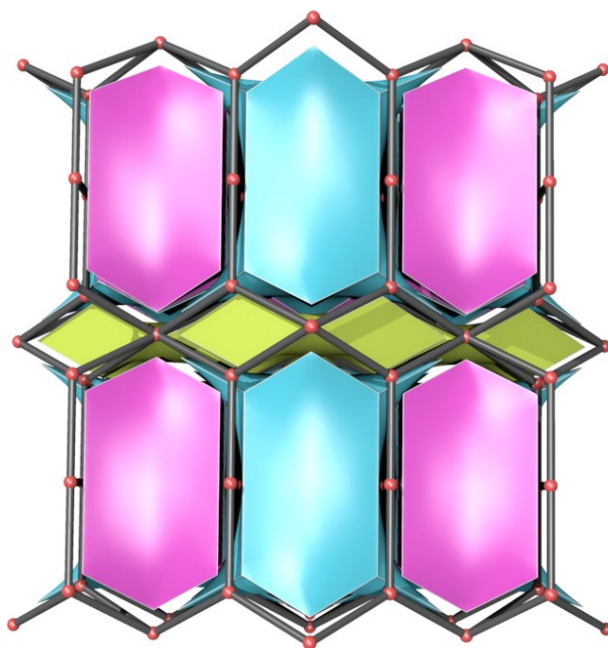


**Figure S11.** The simplified topology of PCP-31 by two different methods.

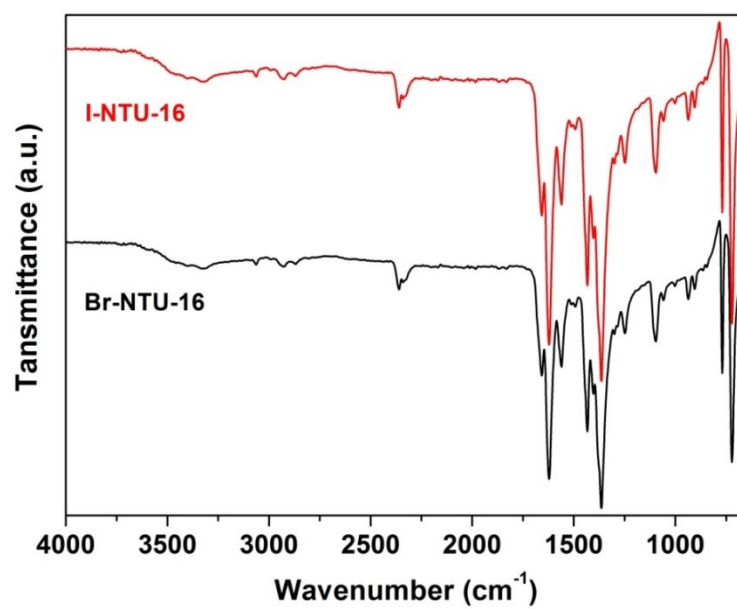


**Figure S12.** IR of as-synthesized Br-NTU-16 and I-NTU-16.

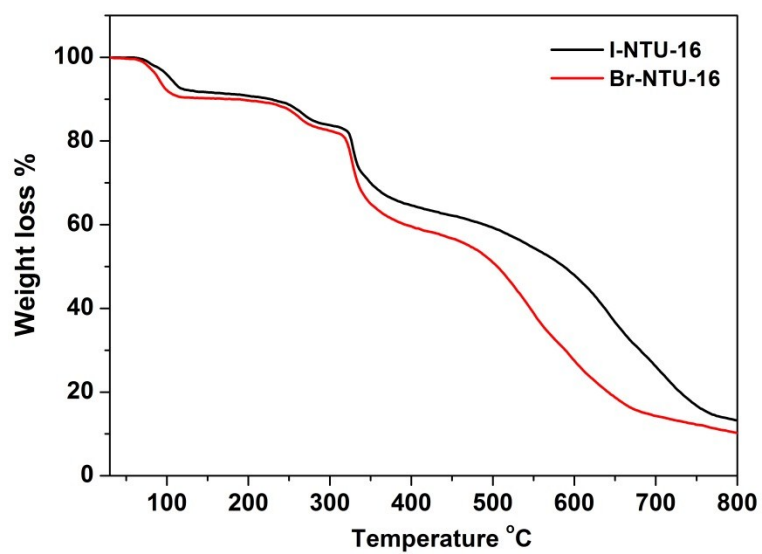


**Figure S13.** TG of as-synthesized Br-NTU-16 and I-NTU-16.

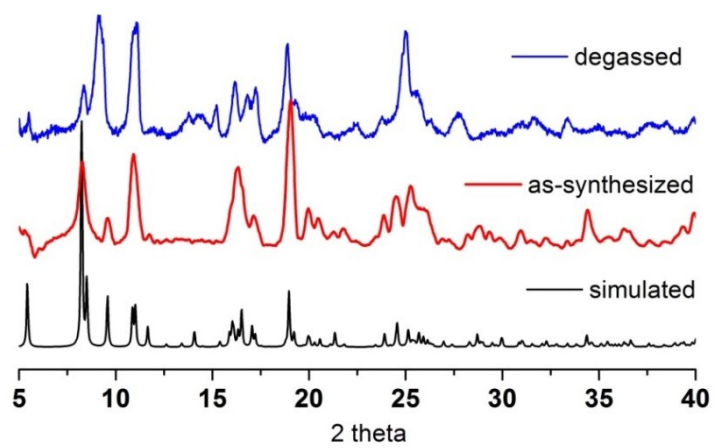


**Figure S14.** PXRD of as-synthesized and degassed Br-NTU-16.

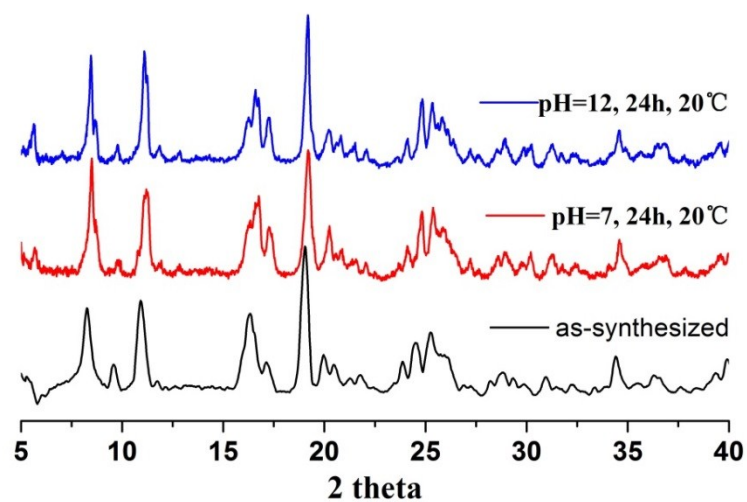


**Figure S15.** PXRD of water and base treated Br-NTU-16.

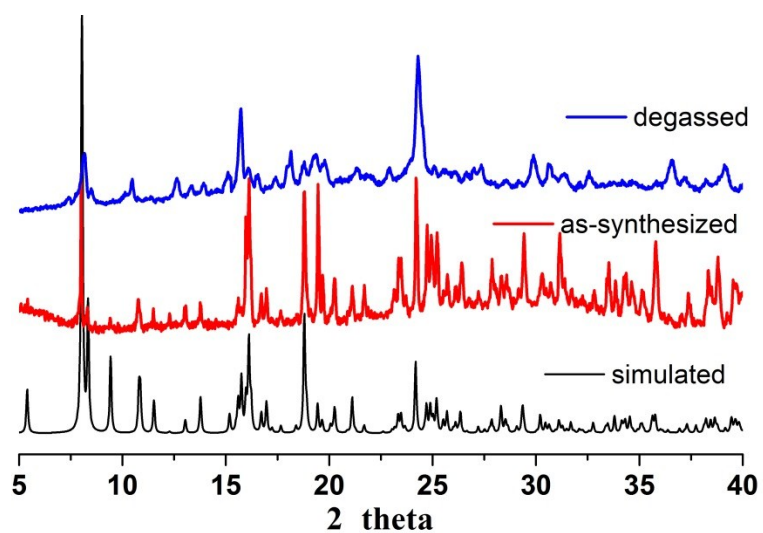


**Figure S16.** PXRD of as-synthesized and degassed I-NTU-16.

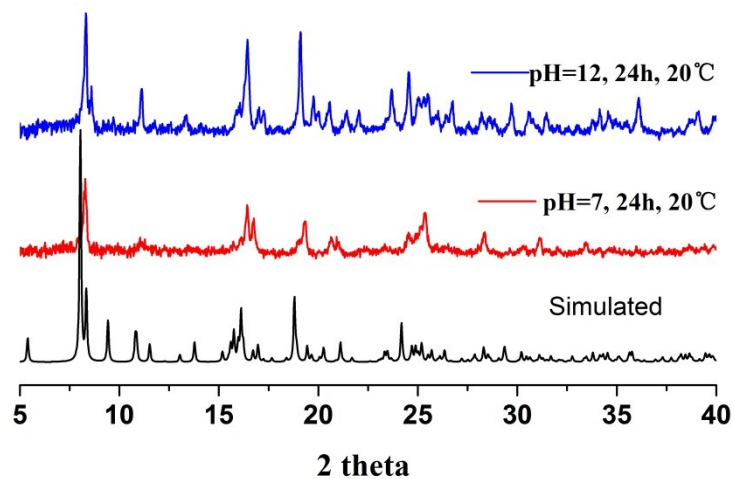


**Figure S17.** PXRD of water and base treated I-NTU-16.

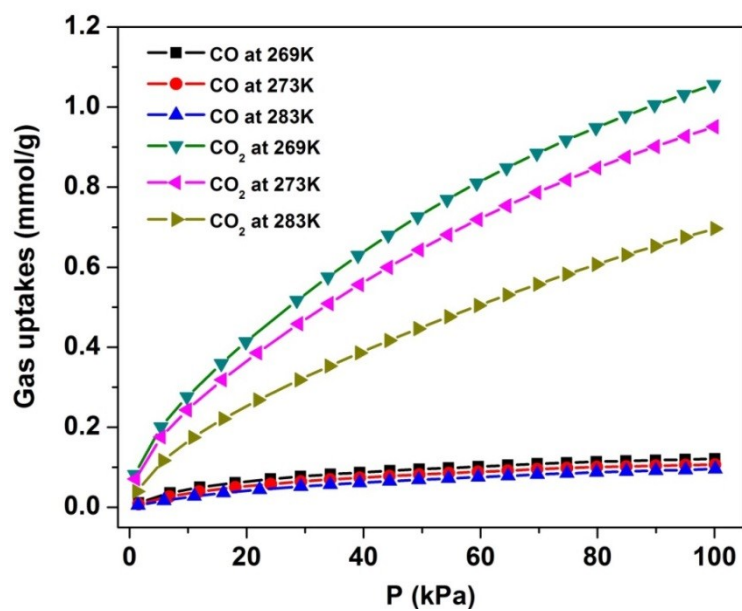


**Figure S18.**  $\text{CO}_2$  and  $\text{CO}$  gas adsorption of Br-NTU-16 at 269, 273 and 283K.



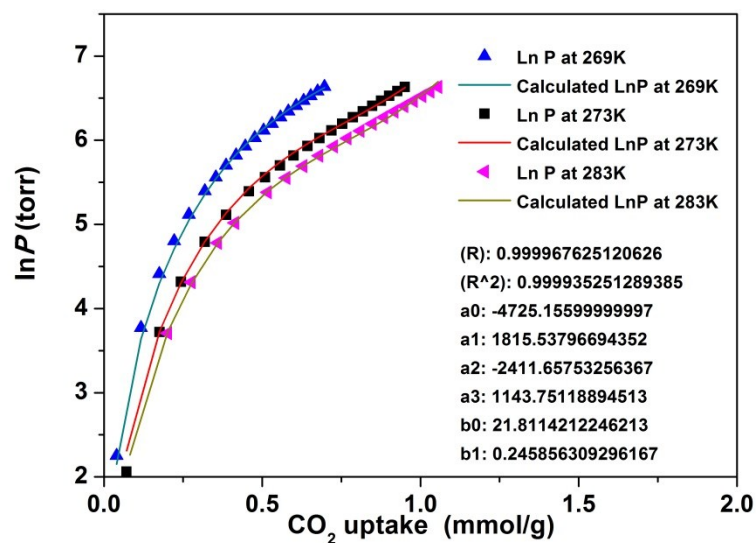


**Figure S19.** The calculated virial equation isotherms parameters fit to the experimental CO<sub>2</sub> data of Br-NTU-16.

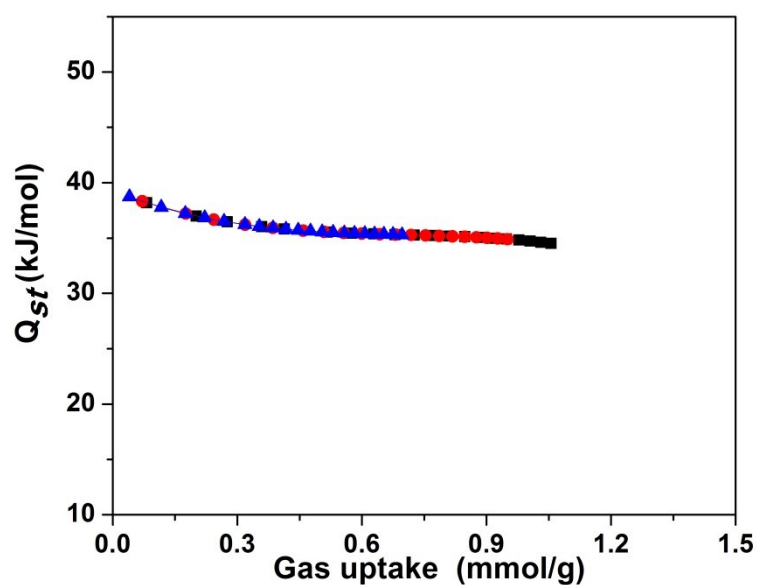


**Figure S20.** Isosteric heat of CO<sub>2</sub> for Br-BTU-16.

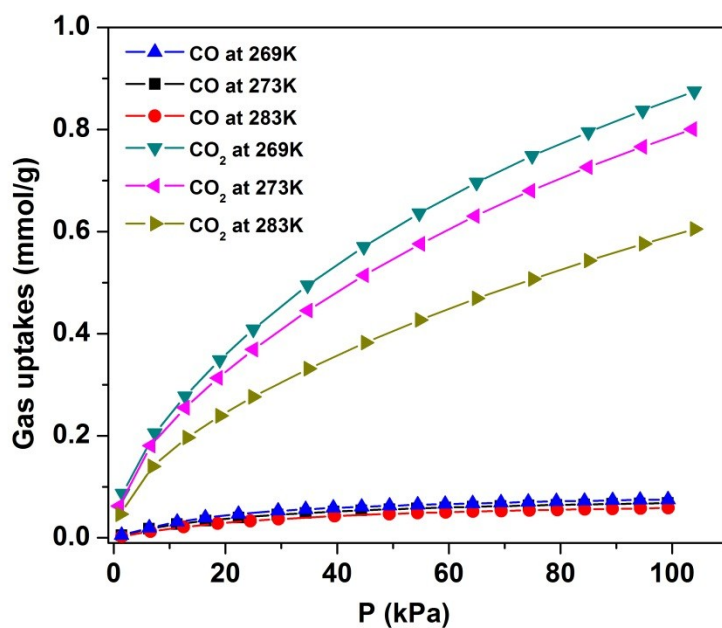


**Figure S21.** CO<sub>2</sub> and CO gas adsorption of Br-NTU-16 at 269, 273 and 283K.

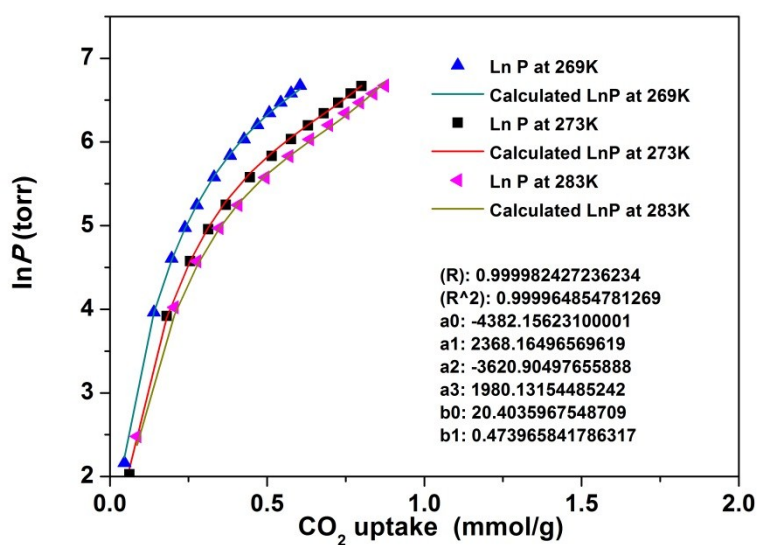


**Figure S22.** The calculated virial equation isotherms parameters fit to the experimental CO<sub>2</sub> data of Br-NTU-16.



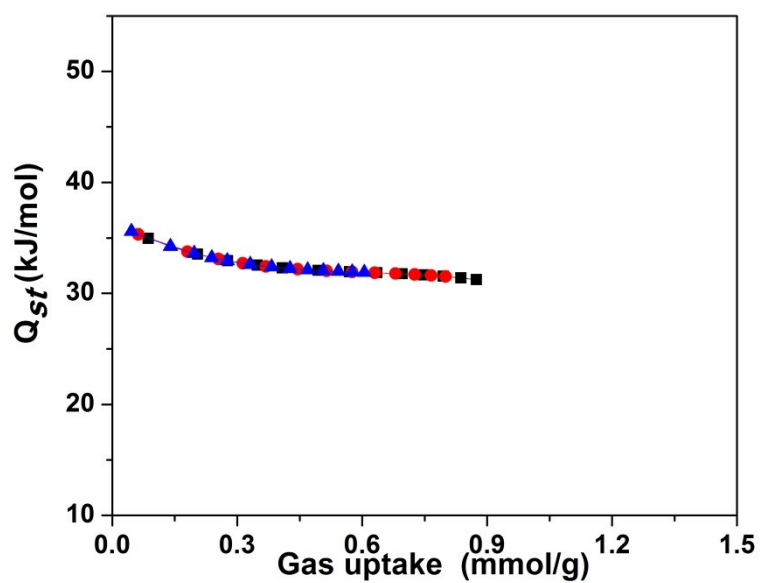


**Figure S23.** Isosteric heat of CO<sub>2</sub> for Br-BTU-16.

**Table S3.** Calculated CO<sub>2</sub>/CO selectivity by Henry's Law in Br-NTU-16 and I-NTU-16.

$K_h$	Br-NTU-16		I-NTU-16	
	CO <sub>2</sub>	CO	CO <sub>2</sub>	CO
269 K	0.014324	0.001086	0.016358	0.000490
273 K	0.011073	0.000861	0.012884	0.000425
283 K	0.006007	0.000496	0.007307	0.000303
CO <sub>2</sub> /CO Selectivity				
269 K	13.2		33.4	
273 K	12.8		30.3	
283 K	12.1		24.1	

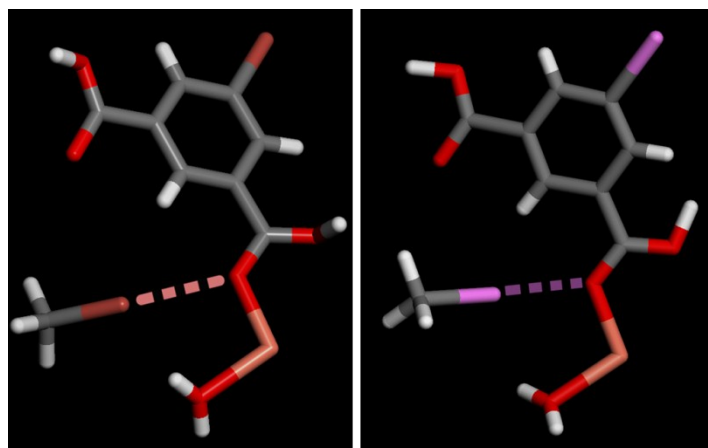


**Figure S24.** Same model systems from Br-NTU-16 (right) and I-NTU-16 (left)

The single-point energy calculations are performed on two model systems (see the above figure) using density functional theory (DFT/B3LYP) method<sup>5,6</sup>. The LanL2dz pseudopotential is used for Br, I, and Cu atoms, and 6-31G basis set for C, H, and O atoms. It is noted from Mulliken atomic charge distribution (Br(17)-O(2): Br(0.026374), O(-0.545903)) that the electrostatic interaction between bromine and carbonyl oxygen is weaker than that of iodine and carbonyl oxygen system (I(2)-O(16) : I(0.113197), O(-0.552390)). Those calculations are consistent well with our experiment data.

**Table S4.** Mulliken atomic charges of the model systems from Br/I-NTU-16

Br-NTU-16		I-NTU-16	
1	O -0.432544	1	C -0.716215
<b>2</b>	<b>O -0.545903</b>	<b>2</b>	<b>I 0.113197</b>
3	Br 0.055769	3	C 0.473573
4	C 0.568913	4	C 0.052466
5	C 0.043002	5	C -0.131302
6	C -0.096923	6	H 0.183901
7	H 0.120696	7	C -0.032339
8	C -0.305815	8	C -0.063419
9	C -0.090793	9	H 0.188534
10	H 0.181883	10	C -0.384668
11	C 0.058156	11	C -0.068986
12	C -0.154222	12	H 0.150290
13	H 0.195860	13	C 0.440895
14	C 0.397991	14	I 0.144434
15	O -0.535026	15	O -0.533552
16	O -0.491819	<b>16</b>	<b>O -0.552390</b>
<b>17</b>	<b>Br 0.026374</b>	17	O -0.502987
18	C -0.609382	18	O -0.399377
19	Cu 0.071641	19	Cu 0.158905
20	O -0.698456	20	O -0.686812

21 H 0.426848	21 H 0.425494
22 H 0.422124	22 H 0.420156
23 H 0.403812	23 H 0.194550
24 H 0.399682	24 H 0.183036
25 H 0.198360	25 H 0.202093
26 H 0.191321	26 H 0.326768
27 H 0.198454	27 H 0.413755

1. G. M. Sheldrick, *Acta Crystallogr. Sec. A*, 2008, **64**, 112-122.
2. (a)P. Vandersluis and A. L. Spek, *Acta Crystallogr. Sec. A*, 1990, **46**, 194-201; (b)A. L. Spek, *J. Appl. Crystallogr.*, 2003, **36**, 7-13.
3. J. G. Duan, Z. Yang, J. F. Bai, B. S. Zheng, Y. Z. Li and S. H. Li, *Chem. Commun.*, 2012, **48**, 3058-3060.
4. A. Saeed, M. Qasim and J. Simpson, *Acta Crystallogr. Sec. C*, 2013, **69**, 790-791.
5. V. Tran, Q. Tran, and M. Hendrickx, *J. Phys. Chem. A*, 2015, **119**, 5626–5633.
6. T. D. Hang, H. T. Nguyen, and M. T. Nguyen, *J. Phys. Chem. C*, 2016, **120**, 10442–10451